Evolution of the decay of highly excited nuclei

H.-Y. Wu, G.-X. Dai, G.-M. Jin, Z.-Y. Li, L.-M. Duan, Z.-Y. He, W.-X. Wen, B.-G. Zhang, Y.-J. Qi, Q.-Z. Luo, and Z.-K. Li

Institute of Modern Physics, Chinese Academy of Science, P.O. Box 31, Lanzhou 730000, People's Republic of China

(Received 21 February 1997)

The two-fragment angle correlation functions of mass-symmetric ternary fragment events from highly excited nuclei produced in $^{40}Ar+^{209}Bi/^{197}Au/^{159}Tb/^{115}In$ reactions at 25 MeV/nucleon are used to extract the mean time interval in cascade emissions (τ) of intermediate mass and heavy mass fragments (mass number greater than 20). It is shown that the mean time interval decreases from the characteristic time $\tau=2000-1000$ fm/c for the Ar+Bi and Ar+Au reactions to $\tau=750$ fm/c for the Ar+Tb reaction and to $\tau=50$ fm/c for the Ar+In reaction. The decay mode of hot nuclei evolves from cascade fission to simultaneous multifragmentation as the excitation energy increases and the mass of hot nuclei decreases. [S0556-2813(98)05006-7]

PACS number(s): 25.70.Gh, 25.70.Pq

I. INTRODUCTION

The decay of excited nuclei, formed in heavy ion fusion reactions at low energy, is dominated by light particle evaporation and/or fission. When the projectile energy increases up to the intermediate energy region (20–100 MeV/nucleon), highly excited nuclei (hot nuclei) can be formed by incomplete fusion (ICF) reactions in asymmetric nuclear reaction systems and the decay mechanism becomes more complicated. The vanishing of the incomplete fusion peak for Ar-induced reactions at 44 MeV/nucleon from the folding angle of binary fission [1] does not mean that highly excited compoundlike nuclei do not exist, but it infers the onset of a new decay mode that leads to the production of several large fragments. This decay mechanism is quite different from the standard evaporation and/or fission modes. Thus, the properties and decay mechanisms of hot nuclei have become an important issue to be studied.

It has been observed that nuclear systems at high excitation energy decay via multiple emission of intermediate mass fragments (IMF's, $3\leqslant Z\leqslant 20$) [2–8]. Recently, much attention has been paid to derive the time scales involved in nuclear fragmentation. The studies on fragment-fragment space-time correlation such as two-fragment angle correlation functions and two-fragment velocity correlation functions have been applied to trace the decay evolution of hot nuclei from a cascade process at low excitation energies to a simultaneous multifragmentation process at high excitation energies [9–17]. However, the study of the multifragmentation of hot nuclei (nuclear matter is kept as nuclei for a period of time and reaches thermalized equilibrium) is more important. It is believed that such studies could help us to enhance the understanding of fundamental properties of nuclei under extreme conditions.

The mechanism of multifragment emission is one of the key issues in the study of hot nuclei decay. The process of multifragment emission can be explained theoretically by a cascade model [18,19] or by a simultaneous multifragmentation model [20,21]. However, within some reasonable range of adjustable parameters, both of those two extreme theories can reproduce experimental mass distributions and multiplicity of the emitted particles. The essence of the decay of hot nuclei has not been clearly discussed within those two models so far. A more realistic decay mode was suggested in Refs. [9,13,15], that is, a cascade decay at low excitation energy and a simultaneous decay at high excitation energy.

Recently, we have studied mass-symmetric ternary fragment events and we have focused on the decay of a transition region from high excitation to low excitation energies. Evidence that mass-symmetric ternary fragment events exist in hot nuclei decays in this excitation energy region has been obtained. The relative angles and velocities of fission fragments have been measured in the $^{12}C+^{197}Au$ reaction at 47.5 MeV/nucleon [22]. An excitation function of ternary fragment events (the ratios of ternary fragment events to binary fission events) has been measured in the $^{12}C+^{209}Bi$ reaction [23]; the excitation function has been successfully reproduced by a statistical cascade model without any adjustable parameters [26]. The deformation potentials of ternary fission by cascade, oblate, and prolate modes have been compared [24,25]; the most probable cascade fission mode has been shown. Cascade emission has been confirmed in Ar +Au/Bi/Tb reactions at 25 MeV/nucleon [27,28] in terms of a kinematics analysis [13] for the ternary fragment event that is dominated by Coulomb repulsive force among the exit fragments. Finally, massive four-body events were observed in Ar+Au/Bi/Tb reactions at 25 MeV/nucleon [29].

In this paper, the two-fragment angle correlation functions of mass-symmetric ternary fragment events are used to extract the mean time interval in cascade emissions to directly analyze the decay mechanisms of hot nuclei. The relationship between angular correlation functions and emission time intervals is discussed according to the calculation of Coulomb trajectories. The mean time intervals are obtained for each reaction by comparing the calculated correlation functions with the measured ones in the Ar+Bi/Au/Tb/In reactions at 25 MeV/nucleon. Our experimental analysis shows that cascade decay dominates at an excitation energy of less than 3 MeV/nucleon and the simultaneous multifragment emission dominates at an excitation energy greater than 4.5 MeV/nucleon for the heavy hot nuclei. The correlation functions show that the mean time interval decreases as the excitation energy increases and/or the mass of hot nuclei decreases. The ternary fragment event comes from hot nuclei

produced by central collisions and a space isotropy is shown by orientation of the ternary fragment event plane.

II. SELECTION OF HOT NUCLEI FORMED IN CENTRAL COLLISIONS

The exit channel identification of hot nuclei is complicated in intermediate energy reactions. A mixture of different products coming from different mechanisms and/or from different emitters should be avoided. In order to study the reaction mechanism, collision parameters for the entrance channel and the products from equilibrium or preequilibrium systems should be separated from each other.

A series of experiments, using reactions induced by ^{40}Ar bombarding on ^{209}Bi/^{197}Au/^{159}Tb/^{115}In targets at 25 MeV/nucleon, was performed to study the transition characteristics of hot nuclei from cascade decay to simultaneous decay by mass-symmetric ternary fragment emission. The experiments were carried out at a large cylindrical scattering chamber in HIRFL in Lanzhou using a detection system consisting of 8–14 large area (20×25 cm^2) position sensitive parallel plate avalanche counters (PPAC's) with position resolution of 4 mm (x and y) and time resolution of 0.3 ns. Six PPAC's were symmetrically set at the same polar angle (90° in center-of-mass system) with different azimuthal angles. With this system, we could measure three sets of binary fission and two sets of ternary fragment events. The other two to eight PPAC's were located at different polar angles to extend the detecting range from 45° to 150° and to increase the coincidence efficiency. This experimental setup can avoid measuring threefold fragment events in which the projectilelike fragments (mainly deep-inelastically scattered particles) are followed by standard fission of targetlike fragments.

The mass symmetry for ternary fragment events can be shown by Dalitz plots where a three-body event is represented by a point inside a triangle. The three distances of the point to the sides of the triangle are proportional to the three masses of the fragments. Dalitz plots were calculated using an event generator (Eugene code) [30] to simulate ternary fragment events with different collision parameters. The Dalitz plots for central collisions [Fig. 1(a)] are different from that for peripheral collisions [Fig. 1(b)] in the ^{40}Ar+^{197}Au reaction at 25 MeV/nucleon. The peripheral ternary fragment events mainly contain two large fission fragments from targetlike nuclei and one projectilelike fragment emitted forward with mass number around 40. These events were located near the midpoints of the sides of the triangle. The events, in which fragments were emitted from the highly excited nuclei in a central collision, were plotted at the center of the triangle. The measured ternary fragment events were selected and analyzed. The experimental data shown in Fig. 1(c) show that symmetric ternary fragment emission was identified in the present experiment.

To verify that the fragments are emitted from an equilibrated system, the isotropy of the fragments emitted was determined in their center-of-mass systems as

$$R=\frac{2}{\pi}\frac{\Sigma A_i|V_{i\perp}|}{\Sigma A_i|V_{i//}|}.$$

Here A_i is the deduced mass of fragment i, and $V_{i\perp}$ and $V_{i//}$ are the polar and radial components of the velocities of fragment i, respectively. It has been shown in Ref. [27] that the experimental distribution of R indicates an equilibrium of the momentum distribution of fragments.

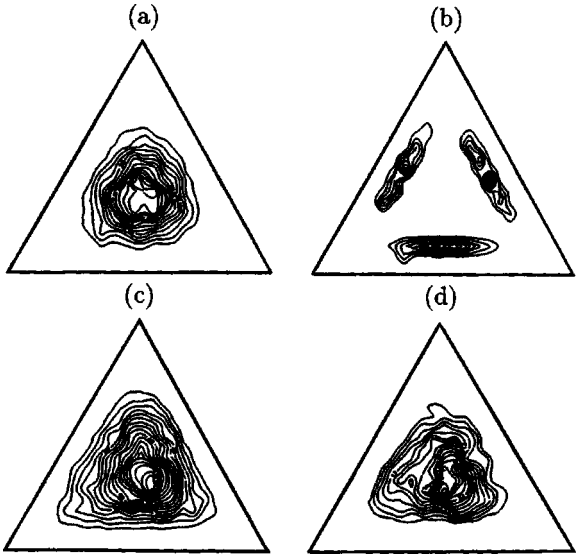

FIG. 1. The calculated Daliz plots (a) for a central collision ($b=2$ fm) and (b) for a peripheral collision ($b=8$ fm) using the Eugene code for the ^{40}Ar+^{197}Au (25 MeV/nucleon) reaction are compared with the experimental plot (c) for the ^{40}Ar+^{197}Au (25 MeV/nucleon) reaction and (d) for the ^{40}Ar+^{209}Bi (25 MeV/nucleon) reaction.

To manifest highly excited nuclei, we have measured the α-particle spectrum at backward angles $\theta=165°$, with $\Delta E+E$ surface barrier gold-silicon telescopes, in coincidence with the binary fission event. The linear momentum transfer (LMT) ratios covered the range of 0.2–1.0, corresponding to a temperature ranging from 3 MeV to 5.4 MeV. The most probable LMT factor was close to 0.85, which corresponds to a nuclear temperature of 4.4 ± 0.5 MeV, in the ^{40}Ar+^{197}Au reaction at 25 MeV/nucleon [31].

The ratio of the probability of ternary fragment event to binary fission increases with increasing excitation energy and decreases with decreasing system mass. The measured values were 4.43% for the ^{209}Bi target, 1.79% for the ^{197}Au target, 0.65% for the ^{159}Tb, and 0.095% for the ^{115}In target, all bombarded by a 25 MeV/nucleon ^{40}Ar beam.

An angular distribution of fission direction of ''ternary fission'' has been defined as the distribution of normal directions of the exit plane of the three fragments. The experimental distribution (histogram in Fig. 2) is compared with the simulated one, filtered by the geometrical acceptance of the detector, in which a space isotropic distribution was assumed (dot in Fig. 2). The agreement between experimental and simulated distributions shows that the orientation of the exit plane of three fragments is independent of the beam direction.

III. CORRELATION FUNCTION FOR CASCADE EMISSIONS

Using the Coulomb minimization procedure [13], we have successfully analyzed the cascade emissions of ternary frag-

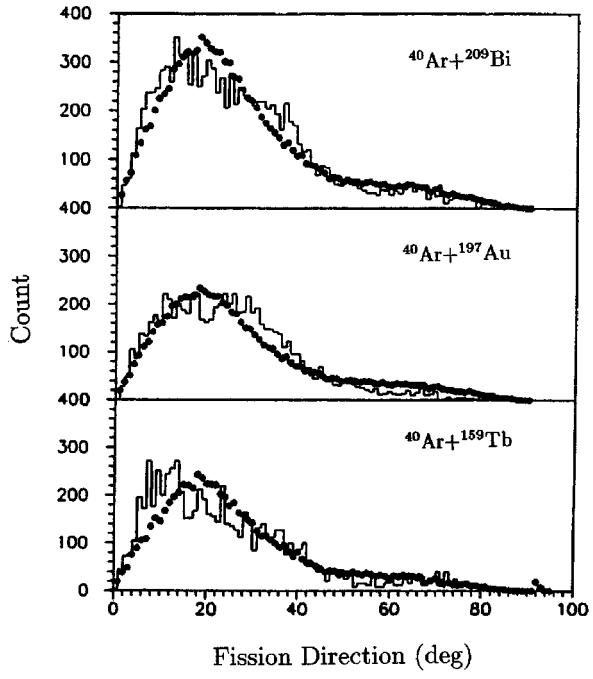

FIG. 2. The experimental angular distributions of the normal line of the ternary fragment plane (histogram) are compared with a simulated value, in which the space isotropic distribution of ternary fragment events is assumed. (Here the angle between normal line of the ternary fragment plane and beam line is used.)

ment events [28], but the time scale of emission was still unknown. To extract the time scale with angular correlation techniques, one needs to reconstruct the experimental correlation function and to calculate the correlation functions for different emission time scales.

The relative angles of two fragments need to be reconstructed in the center-of-mass system of the ternary fragment event, the correlative spectrum is obtained by summing up all pairs of fragments. The experimental distribution of the relative angle should be peaked at 120°. In fact, the simulated distributions show a peak at 120° for both the cascade ternary fragment events and simultaneous ones. This peak was sharpened by the experimental setup. An angular correlation function, which is independent of detector geometrical acceptance, was defined as the ratio of two distributions:

$$R(\theta_{ij}) = \frac{Y_{\mathrm{cor}}(\theta_{ij})}{Y_{\mathrm{uncor}}(\theta_{ij})},$$

where θ_{ij} is the relative angle, $Y_{\mathrm{cor}}(\theta_{ij})$ is the measured normalized angular distribution (or simulated one) with a characteristic time interval, and $Y_{\mathrm{uncor}}(\theta_{ij})$ is the simulated one for uncorrelated events, respectively. All the simulated distributions were filtered by the geometrical acceptance of the detectors.

The uncorrelated events are supposed to be two successive binary splittings, in which there is no interaction between the fragments of the first and of the second splitting. In other words, the time interval of two splittings is much longer than the time necessary for the first fragment to escape from the main Coulomb field of the residue part. A typical case is that of fragments, say, F1 and F2, coming from the first splitting, and fragments F3 and F4, coming from the second splitting of nuclei F1. The axes of each splitting are randomly oriented in the center-of-mass system of the hot nuclei and the masses of F2, F3, and F4 are determined from the experimental mass distribution. The uncorrelated events could be generated by taking into account the Coulomb velocities and recoil effect. Events with a characteristic time interval were produced and the angles of the exit fragments were obtained by tracking the trajectory, by assuming that the kinetic energy at the scission point is zero and the relative motion of the splitting fragments is decided by the Coulomb repulsive force.

The kinematic trajectories of the emitted fragments were analyzed, when the Coulomb action in the final state with a characteristic emission time (τ) was taken into account. At the beginning of a decay process, the initial nuclear system (at the first splitting) was composed of three fragments with experimental mass and with spherical shape. The three-ball system had at least two touching points. The positions of the fragments and their emission mode were simulated with a Monte Carlo method. First, one fragment escaped and the residual two balls were split at a time interval t, where t was given by a probability distribution $P(t)=(1/\tau)e^{-t/\tau}$. The kinematics of fragment trajectories were calculated by solving the differential equation of motion including rotations.

The essence of the angular correlation function is a deviation of the fragment-emitting directions due to the mutual Coulomb action. If the emitted three fragments are closer, the deviations become larger. This correlation is related to two factors: one is the relative position of emitted fragments that is determined by the free parameter of emission time and initial position; the other is the mutual forces among the splitting fragments that are determined by the mass and charge of the fragments. The correlation function only depends on the masses of the initial nuclei, on the mass symmetry of the ternary fragment event, and on the time scale for emission. It is independent of the excitation energy or the temperature of the hot nuclei that determine the probabilities of mass-symmetric ternary fragment events.

IV. TRANSITION FROM CASCADE TO SIMULTANEOUS DECAY

The evolution of the emission mode can be understood by studying the evolution of the correlation function with the mean time interval in fragmentation emissions. In our case, the time interval ranges from 0 fm/c to 2000 fm/c where the longer time is related to cascade emission and the shorter time is related to simultaneous emission. The calculated correlation functions show that the method of measurement correlation functions is moderate when the measured mean time interval is in the range from 0 fm/c to 2000 fm/c. For a time interval longer than 2000 fm/c, the multifragment events are associated with uncorrelated events. The events in which the mean time interval is less than 100 fm/c exhibit a strong Coulomb interaction among fragments. In this situation, a simultaneous decay is thought to occur.

The simulated correlation functions are represented in Figs. 3 to 6 by histograms in different frames with the mean time interval in cascade emissions, τ indicated in the frame. The experimental correlation functions are displayed as open dots with an error bar. One can notice that the shapes of the correlation functions are independent of the τ for both small

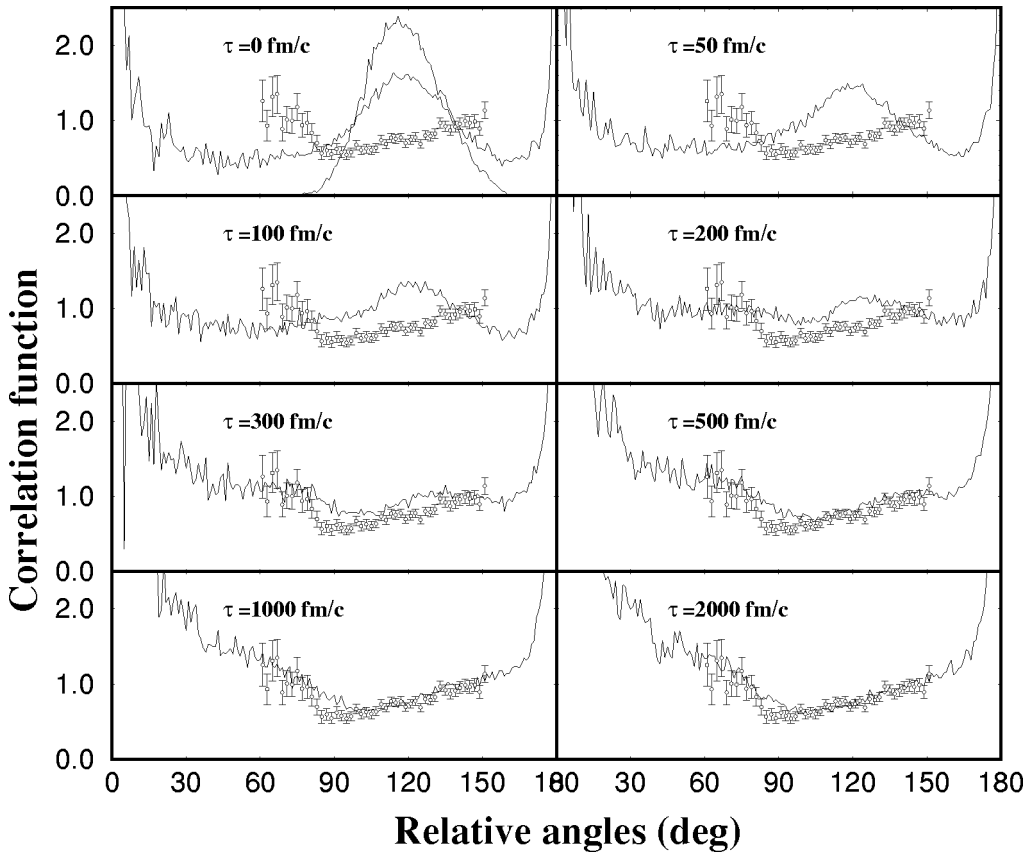

FIG. 3. The measured angular correlation function of fragments for ^{40}Ar+^{209}Bi (open circles with error bar) is compared with a simulated one with a different mean time interval in cascade emissions. The mean time intervals are indicated in each frame.

and large relative angles. A difference from Ref. [13] is due to different definitions of the correlation function. Using our experimental data, the shapes of correlation functions strongly depend on the τ in the angular range of 60°–160°, allowing the extraction of time information on the fragment-emission process. For short $\tau(\tau \leqslant 100$ fm/$c)$, we find a ''positive'' correlation. A Gauss-like distribution with a sharp peak at $\tau=0$ fm/c is obtained. The distributions of τ at 200–300 fm/c tend to be flat. For large $\tau(\tau \geqslant 500$ fm/$c)$, a ''negative'' correlation is shown. The best measured range to extract τ is therefore the τ-sensitive range of $0-500$ fm/c.

In the ^{40}Ar-induced collisions at 25 MeV/nucleon with ^{209}Bi/^{197}Au/^{159}Tb/^{115}In targets, hot nuclei are assumed to be formed in central collisions. The two-fragment angle correlation functions of mass-symmetric ternary fragment events show that the correlation functions give $\tau=2000^{+1000}_{-1000}$ fm/c for the ^{40}Ar+^{209}Bi reaction (Fig. 3), $\tau=1000^{+1000}_{-700}$ fm/c for the ^{40}Ar+^{197}Au reaction (Fig. 4), $\tau=750^{+200}_{-200}$ fm/c for the ^{40}Ar+^{159}Tb reaction (Fig. 5), and $\tau=50^{+30}_{-20}$ fm/c for the ^{40}Ar+^{115}In reaction (Fig. 6). The large errors are resulting from the fact that the correlation functions are not sensitive to this time scale in Ar+Au and Ar+Bi systems. As the mass of the target decreases, as the excitation energy of hot nuclei increases, and as the mass of hot nuclei decreases in the present case, the transition behavior for multifragment decay evolves from cascade splitting to simultaneous multifragmentation.

The cascade decay occurs naturally when the excitation energy cannot be totally taken away by one decay of the excited nucleus. If the mean time interval τ is longer than the time of deformation of normal binary fission, a cascade fission mode occurs. The cascade fission can be treated with a statistical model for hot nuclei at low temperature [26]. One can find that the probability of cascade fission increases, as the fragment mass of the first splitting increases and the surviving excitation energy of the fragment also increases. When the temperature of hot nuclei increases, the width of the mass distribution of fission fragments grows and the residual excitation energy increases. It is well known that a lot of intermediate mass fragments are emitted from hot nuclei, and the IMF mass increases when the temperature increases. If we take the heavy IMF emission as a first splitting and the sequential fission of residues as the second splitting, mass-symmetric cascade fission should take place.

The three possible modes for ternary fission are cascade fission, oblate ternary fission, and prolate ternary fission. Their deformation potentials were calculated with suitable one-, two-, and three-axis deformations including Coulomb potential, surface energy, shell energy, and nuclear potential [25]. The simulated barrier of 150 MeV (for the $^{234}_{96}$Cm nucleus, at a temperature $T=2$ MeV) for the oblate mode is remarkably higher than that of the cascade mode and prolate mode. However, the oblate mode is one of the open decay channels of hot nuclei because the excitation energy is higher than the barrier.

As the excitation energy increases, the cascade emission

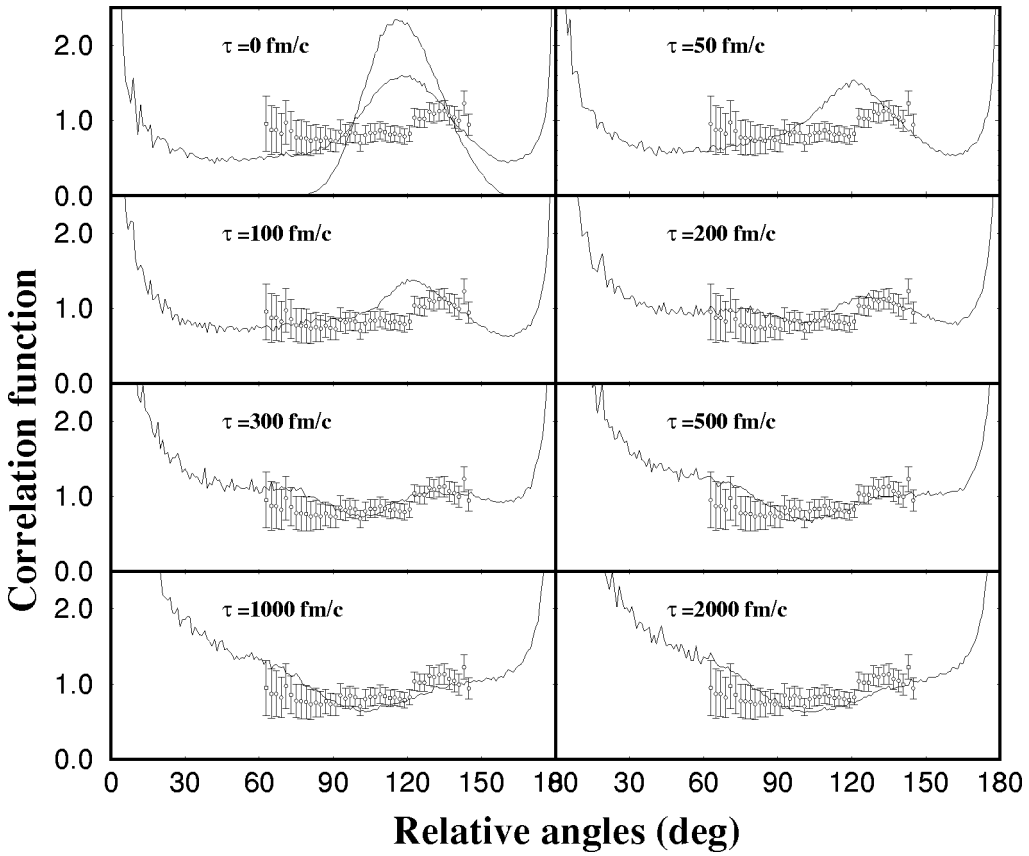

FIG. 4. The angular correlation functions for the $^{40}Ar+^{197}Au$ reaction (same as Fig. 3).

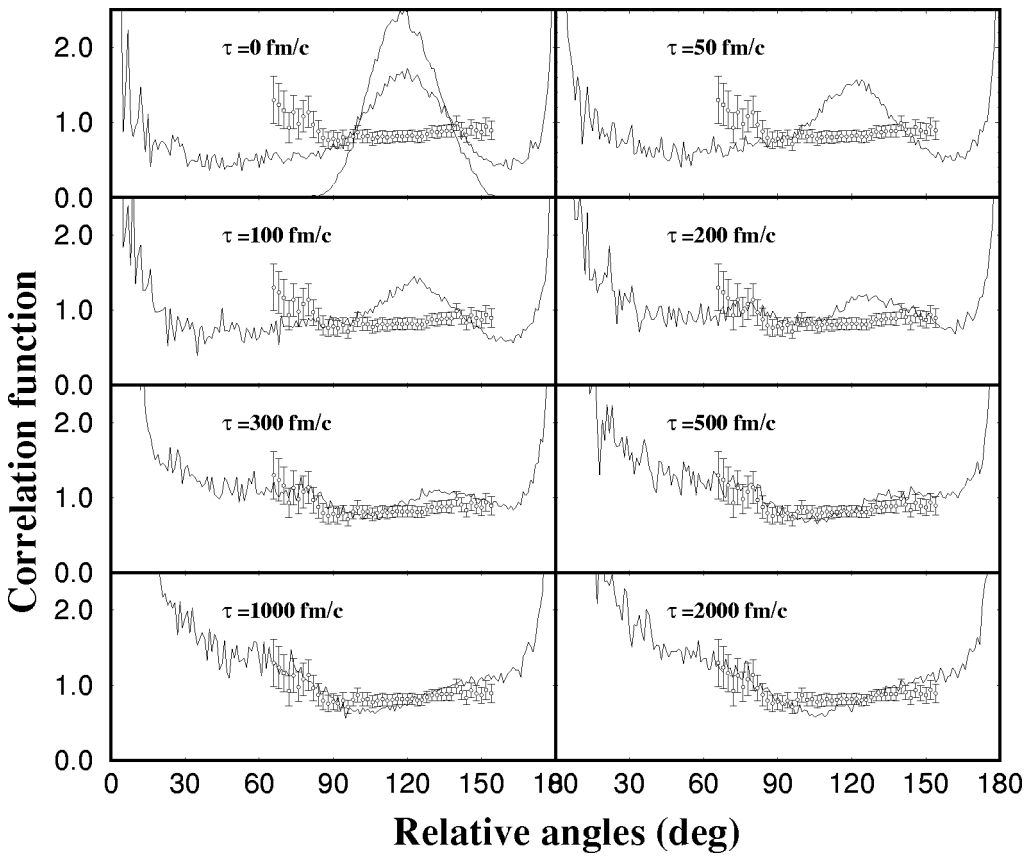

FIG. 5. The angular correlation functions for the $^{40}Ar+^{159}Tb$ reaction (same as Fig. 3).

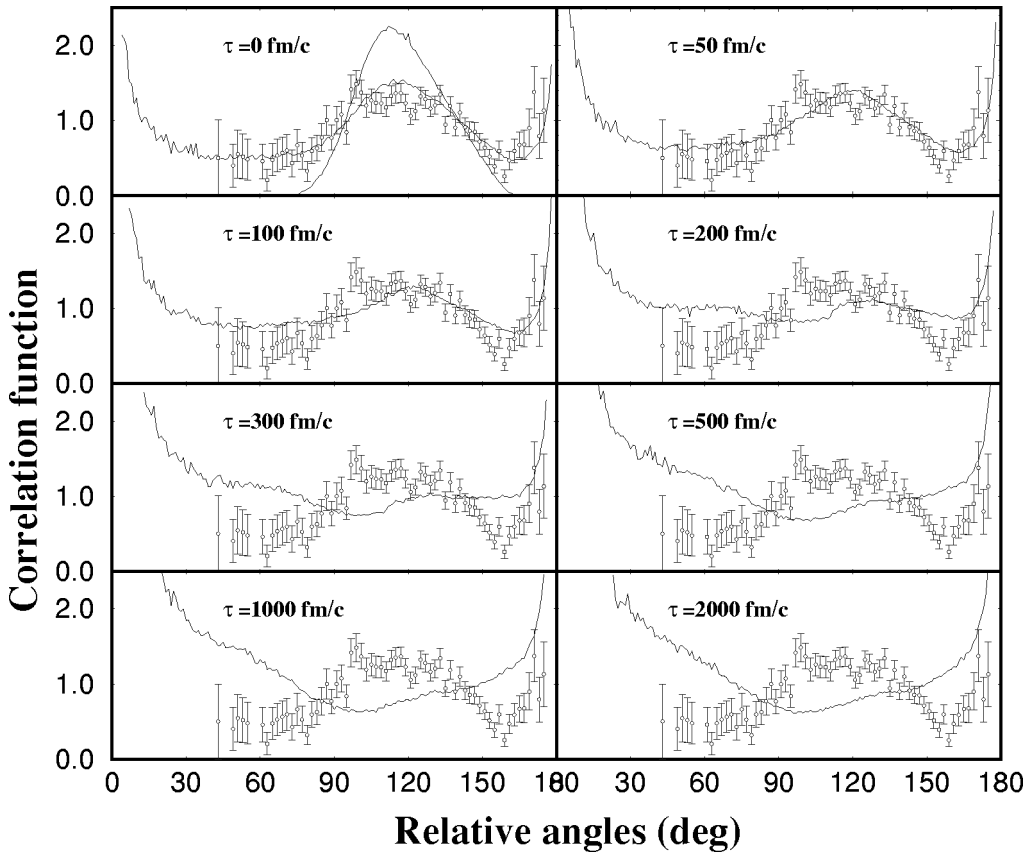

FIG. 6. The angular correlation functions for the $^{40}Ar+^{115}In$ reaction (same as Fig. 3).

time reduces and the decay mode evolves from cascade decay to simultaneous decay. When the time is less than the deformation time of normal binary fission, a multiple-axis deformation of hot nuclei takes place. Mass-symmetric ternary fission is therefore suggested to take place in hot nuclei.

V. CONCLUSION

The mass-symmetric ternary fragment events, which come from hot nuclei with mass $A=130–220$, show a space isotropy orientation in the exit plane of ternary fragment events. The two-fragment angle correlation functions of the events are used to extract the mean time interval τ. τ decreases from 2000 to 1000 fm/c for the $^{40}Ar+^{209}Bi$ and $^{40}Ar+^{197}Au$ reactions, to 750 fm/c for the $^{40}Ar+^{159}Tb$ reaction, and to 50 fm/c for the $^{40}Ar+^{115}In$ reaction with beam energy at 25 MeV/nucleon.

When the excitation energy of excited nuclei is less than or equal to 3 MeV/nucleon, mass-symmetric ternary fragment events take place. Those events are mainly caused by an asymmetric splitting of hot nuclei followed by a splitting of the large fragment. We have shown that the higher the temperature of the excited nuclei, the shorter the mean time interval of the sequential splitting. With increasing excitation energy and/or decreasing the mass of hot nuclei, the mean time interval decreases. When it decreases to a value of 200 fm/c or even smaller, the decay mode evolves to a simultaneous decay.

It is suggested that mass-symmetric ternary fission is produced by cascade fission at low temperature in hot nuclei. When the ternary fission evolves to simultaneous oblate ternary fission and/or prolate ternary fission at high temperature, a multiple-axis deformation of hot nuclei is implied.

ACKNOWLEDGMENTS

This work is supported by the National Natural Science Foundation of China under Grants No. 19505007, 19175053, 19275054, and 19675053. The authors would like to express appreciation to the staff of HIRFL at the Institute of Modern Physics for providing the good experimental conditions.

[1] E. C. Pollacco *et al.*, Phys. Lett. **146B**, 29 (1984).
[2] J. E. Finn *et al.*, Phys. Rev. Lett. **49**, 1321 (1982).
[3] J. W. Harris *et al.*, Nucl. Phys. **A471**, 241c (1987).
[4] C. A. Ogilvie *et al.*, Phys. Rev. Lett. **67**, 1214 (1991).
[5] R. T. de Souza *et al.*, Phys. Lett. B **268**, 6 (1991).
[6] D. R. Bowman *et al.*, Phys. Rev. Lett. **67**, 1527 (1991).
[7] W. Bauer, G. F. Bertsch, and S. Das Gupta, Phys. Rev. Lett. **58**, 863 (1987).
[8] William A. Friedman, Phys. Rev. C **42**, 667 (1991).
[9] G. Bizard *et al.*, Phys. Lett. B **302**, 162 (1993).
[10] R. Bougault, J. Colin, F. Delaunay, A. Genoux-Lubain, A. Hajfani, C. Le Brun, J. F. Lecolley, M. Louvel, and J. C.

Steckmeyer, Phys. Lett. B **232**, 291 (1989).
[11] D. R. Bowman *et al.*, Phys. Rev. Lett. **70**, 3534 (1993).
[12] Y. D. Kim *et al.*, Phys. Rev. Lett. **67**, 14 (1991).
[13] M. Louvel *et al.*, Phys. Lett. B **320**, 221 (1994).
[14] D. Durand *et al.*, Phys. Lett. B **345**, 397 (1995).
[15] E. Bauge *et al.*, Phys. Rev. Lett. **70**, 3705 (1993).
[16] L. Phair *et al.*, Phys. Rev. C **47**, R421 (1993).
[17] E. Cornell *et al.*, Phys. Rev. Lett. **75**, 1475 (1995).
[18] R. J. Charity *et al.*, Nucl. Phys. **A476**, 516 (1988).
[19] D. R. Bowman *et al.*, Nucl. Phys. **A523**, 386 (1991).
[20] D. H. E. Gross, Prog. Part. Nucl. Phys. **30**, 155 (1993); Y. Zheng, H. Massmann, S. Xu, D. H. E. Gross, X. Zhang, Z. Lu, and B. Sa, Phys. Lett. B **194**, 183 (1987); X. Zhang, D. H. E. Gross, S. Xu, and Y. Zheng, Nucl. Phys. **A461**, 668 (1987).
[21] J. P. Bondorf, R. Donangelo, H. Schulz, and K. Sneppen, Phys. Lett. **162B**, 30 (1985); J. P. Bondorf, R. Donangelo, I. N. Mishustin, and H. Schulz, Nucl. Phys. **A444**, 460 (1985); H. W. Barz, J. P. Bondorf, and H. Schulz, Phys. Lett. B **184**, 125 (1987).
[22] Dai Guangxi, Qi Yujin, Luo Qingzheng, Yan Dehong, Cai Wei, Wu Heyu, Zhang Baoguo, Dang Bingrong, and Wen Wanxin, Chin. J. Nucl. Phys. **15**, 101 (1993).
[23] Wu Heyu, Dai Guangxi, Cai We, Qi Yujin, Yan Dehong, Zhang Baoguo, Dang Bingrong, Luo Qingzheng, Qian Xin, and Wen Wanxin, High Energy Phys. Nucl. Phys. **15**, 680 (1993).
[24] G. X. Dai, J. B. Natowitz, R. Wada, Y. N. Lou, K. Hagel, and B. Xiao, Nucl. Phys. **A568**, 601 (1994).
[25] Wu Heyu and Dai Guangxi, Acta Phys. Sin. **43**, 540 (1994).
[26] Wu Heyu and Dai Guangxi, High Energy Phys. Nucl. Phys. **18**, 729 (1994).
[27] Dai Guangxi, Wu Heyu, Jin Genming, Qi Yujin, Li Zhuyu, Duan Liming, He Zheyong, Luo Qinzheng, Wen Wanxin, and Zhang Baoguo, High Energy Phys. Nucl. Phys. **18**, 22 (1994).
[28] Wu Heyu and Dai Guangxi, High Energy Phys. Nucl. Phys. **18**, 5 (1994).
[29] G. X. Dai, H. Y. Wu, Z. Y. He, Q. Z. Luo, L. M. Duan, B. G. Zhang, Y. J. Qi, Z. Y. Li, G. M. Jin, and W. X. Wen, Nucl. Phys. **A583**, 173c (1994).
[30] D. Durand, Nucl. Phys. **A541**, 266 (1992).
[31] H. Wu, G. Jin, Z. Li, G. Dai, Y. Qi, Z. He, Q. Luo, L. Duan, W. Wen, and B. Zhang, Nucl. Phys. **A617**, 385 (1997).